Open questions in baryon spectroscopy

Volker Credé

Institut für Strahlen- und Kernphysik, University of Bonn, Germany

Abstract. The investigation of the excitation spectrum of nucleons provides important information on many open questions in baryon spectroscopy. The key to any progress is the identification of the effective degrees of freedom leading to a qualitative understanding of strong QCD. The problem of *missing resonances* predicted by quark models and the nature of the nucleon resonance $S_{11}(1535)$ is discussed on the basis of recent experimental results of the CB-ELSA experiment at the e^- accelerator ELSA in Bonn. Among other things, the data show clear structures due to high-mass resonance production. Successive decays via $\Delta(1232)\pi$ are observed. The study of symmetries among negative-parity baryons allows predictions of Δ^* decay properties and, therefore, will shed some light on the rather unknown Δ spectrum.

At present, QCD does not account for quark confinement. However, flavor symmetry seems to play a striking role in the confinement of three quarks. This is well observed for the first (u,d) quark family and predictions are also made for the second family (s). Open questions remain as to what the role of the gluon is, for instance.

INTRODUCTION

Quantum chromodynamics (QCD) is almost without doubt the correct theory of strong interaction. However, the QCD Lagrangian cannot be solved yet in the low-energy regime and for bound states, i.e. to provide the theory of quark confinement. In order to describe and to predict the properties of hadronic states, quark models have been developed instead, which are amazingly successful. It is important to complete the predicted spectra and to classify observed particles as well as to understand their properties within the quark model. Any serious discrepancy between the model and the experimental findings may contribute to elucidate the current uncertainties on QCD.

All constituent quark models can roughly be classified in three different categories:

- **Non-relativistic quark models**: Among others, Gloszman and Riska have developed a model treating quarks as q^3 bound states coupling to mesonic fields. These meson-exchange models are more generally also called Goldstone-boson exchange models. The authors use the exchange of an octet of pseudoscalar mesons [1]. The quarks are assumed to be Pauli spinors, thus obeying the Pauli principle. Consequently, bound states can suitably expanded in a basis of non-relativistic wave functions.

- ***Relativised* quark models**: Another group of models still follows a non-relativistic Ansatz but uses the relativistic terms of the energy for the quarks and, furthermore, applies momentum-dependant relativistic corrections to the confining and short-distance potentials [2].
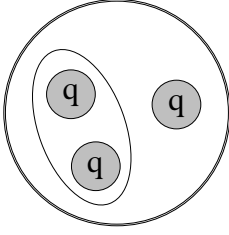
FIGURE 1. Possible quark-diquark structure of the baryon
If one of the internal degree of freedom was frozen, the consequence would be a smaller number of expected baryon resonances.

- **Fully Relativistic quark models**: A relativistically covariant description treats the quarks as full Dirac spinors [3]. The residual interaction is based on instanton-induced forces.

All current models describing the spectrum of baryon resonances predict a series of hitherto unobserved states. This feature would clearly be a big problem for all models as they would have failed to describe physical reality. There are at least two possible explanations which account for this open question. One is that these *missing resonances* have to exist if the 3 valence quarks of the nucleon are not frozen into a quark-diquark substructure. In fact, this would reduce the number of effective degrees of freedom and, therefore, also the number of possible baryon states [4] (Fig. 1).

An alternative explanation is that those *missing resonances* are really missing and have simply not been observed up to now because almost all existing data result from πN elastic-scattering experiments. As a matter of fact, some models focussing on baryon strong decays predict baryon states missing in πN elastic-scattering analyses but showing strong evidence in electromagnetic production [5]. These models create a $q\bar{q}$ pair with vacuum quantum numbers, i.e. quark and antiquark necessarily have relative $L = 1$ and $S = 1$ combined to $J^{PC} = 0^{++}$, and are generally referred to as the $^3P_0$ model [6]. Those *missing resonances* should couple strongly to channels like $\Delta\pi$, for instance [7]. Thus, photoproduction experiments offer a large discovery potential.

Photoproduction of two pseudoscalar mesons off the proton

The observation of baryon resonances in their sequential decay into $p\pi\pi$ is, therefore, particularly suited in photoproduction of $\pi^0\pi^0$ since the latter is not dominated by diffractive scattering of ρ mesons produced by conversion of the incoming photon in the field of the proton. This process dominates the $p\pi^+\pi^-$ channel, especially at high energies. Another dominant contribution in the reaction involving charged pions is the direct production of $\Delta^{++}\pi^-$ (Kroll-Rudermann term). This effect is also excluded in the $p\pi^0\pi^0$ channel.

The study of the reaction $\gamma p \rightarrow p\pi^0\eta$ also allows one to carry out a general search for baryon resonances. These can be Δ excitations decaying into $\Delta(1232)\eta$, for instance. In the following, a deeper interest in the study of this reaction is motivated.

The $N(1535)S_{11}$ has a strong decay mode into $N\eta$ with a branching ratio of (30-55) % while the $N(1650)S_{11}$ hardly decays to $N\eta$. The question arises why this is the case. In Table 1, the negative-parity resonances form isospin groups and are arranged according to their spins. In the quark model, the $N(1535)S_{11}$ and the $N(1520)D_{13}$ are

TABLE 1. Negative-parity baryons and decays into ground state + η

For N* and Λ*, a spin flip is required for the decay of interest from states with $s = \frac{3}{2}$. Therefore, the decay is suppressed. See text for details.

$s = \frac{3}{2}$	$N(1650)S_{11}$	$N(1700)D_{13}$	$N(1675)D_{15}$
$s = \frac{1}{2}$	$N(1535)S_{11}$ → Nη	$N(1520)D_{13}$	

$s = \frac{3}{2}$	$\Lambda(1800)S_{01}$	$\Lambda(????)D_{03}$	$\Lambda(1830)D_{05}$
$s = \frac{1}{2}$	$\Lambda(1670)S_{01}$ → Λη	$\Lambda(1690)D_{03}$	

$s = \frac{3}{2}$	$\Sigma(1750)S_{11}$ → Ση	$\Sigma(????)D_{13}$	$\Sigma(1775)D_{15}$
$s = \frac{1}{2}$	$\Sigma(1620)S_{11}$	$\Sigma(1670)D_{13}$	

$s = \frac{3}{2}$	$\Delta(1900)S_{31}$	$\Delta(1940)D_{33}$ → Δη	$\Delta(1930)D_{35}$
$s = \frac{1}{2}$	$\Delta(1620)S_{31}$	$\Delta(1700)D_{33}$	

approximately mass degenerate and form a doublet of states with $s = \frac{1}{2}$. However, the quarks may also couple to $s = \frac{3}{2}$ resulting in three states corresponding to the observed resonances $N(1650)S_{11}$, $N(1700)D_{13}$ and $N(1675)D_{15}$. Different contradictory arguments try to explain the strong coupling of the $N(1535)S_{11}$ to the Nη decay mode, some even arguing that no genuine three-quark resonance is necessary at all [8, 9]. This conjecture is supported by an amplitude analysis of η production data in which no pole is needed for the $N(1535)S_{11}$ [10]. As a matter of fact, the question as to what the true nature of the resonance is, continues to remain. The systematics of η decays of negative-parity baryons may help to discriminate the proposed models (Tab. 1). The same striking decay pattern as for the nucleons can be found for the Λ resonances where the $\Lambda(1670)$ decays strongly into Λη whereas almost no η decay mode can be observed from the state $\Lambda(1800)$. In the case of the Σ baryons, the situation is reversed. The lower-mass state $\Sigma(1620)$ does not decay into Ση, however, the decay is also forbidden by phase space. Furthermore, the isospin wave functions of Λ and Σ have different symmetries which could be the origin of the observed pattern. In the case of N and Λ resonances, the internal total quark spin of the states at lower mass is dominantly $s = \frac{1}{2}$ whereas of the higher-mass states it is $s = \frac{3}{2}$. This means that for the latter decaying into the ground state, a quark spin flip is required which suppresses the decay. Since no predictions for decays of Δ^* resonances into $\Delta(1232)\eta$ exist, one would expect the $\Delta(1940)D_{33}$ to decay dominantly into Δη on the basis of this naive picture.

All existing models have failed to describe a group of negative-parity states in the Δ spectrum around 1900 MeV. However, it has to be pointed out that these states cannot be considered well known. In fact, the investigation of these resonances and their decay properties will shed some light on the rather unknown Δ spectrum.
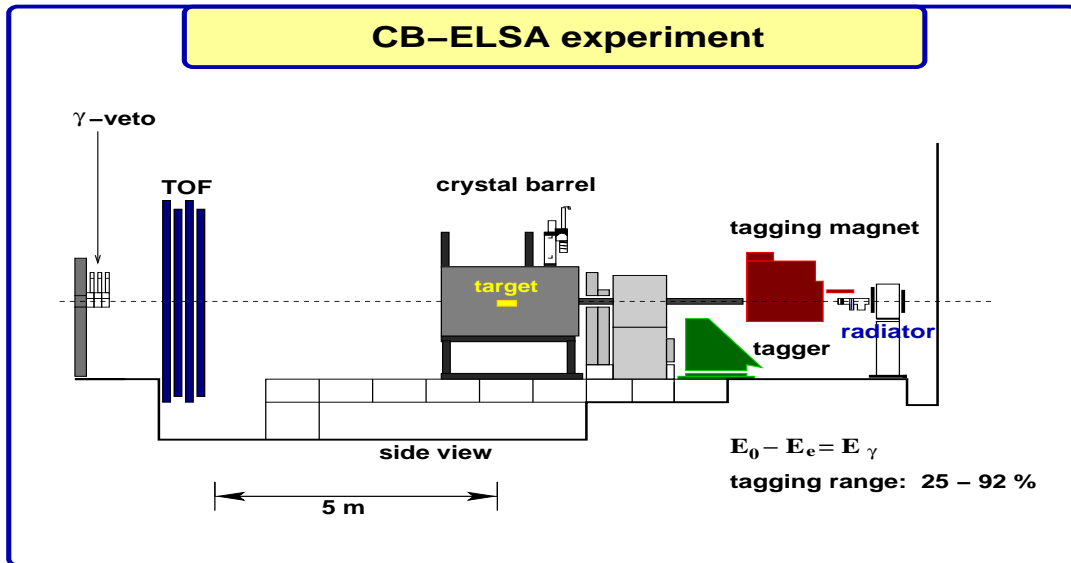
FIGURE 2. Configuration of the CB-ELSA detector for a first series of measurements

THE CRYSTAL-BARREL EXPERIMENT AT ELSA

The ELSA accelerator complex in Bonn provides electron beams up to energies of 3.5 GeV. A LINAC preaccelerates the particles which are then injected into an electron synchrotron. The latter provides electrons up to 1.6 GeV which are finally transferred to the stretcher ring ELSA [11].

The experimental setup of the detector

Electrons extracted from ELSA hit a primary radiation target and produced Bremsstrahlung. The corresponding energy of the photons ($E_\gamma = E_0 - E_{e^-}$) was determined in a tagging system by the deflection of the electrons in a magnetic field. This detector provided a tagged beam in the photon energy range from 25 % up to 95 % of the incoming electron energy. The setup of the CB-ELSA detector used for a first series of experiments is shown in Fig. 2. The calorimeter (Crystal Barrel) consisting of 1380 CsI(Tl) crystals covering about 98 % of 4π solid angle is an ideal detector for photons. The photoproduction target in the center of the Crystal Barrel has a length of 5 cm and was filled with liquid hydrogen. It is surrounded by a scintillating fibre detector which was built to detect and trigger charged particles leaving the target. In addition, it provides an intersection point of a particle's trajectory with the detector and hence helps to identify clusters of charged particles in the barrel. Due to the *in-flight* character of the experiment, the general conception is to combine the calorimeter with suitable forward detectors. In the start configuration, the system was extended by Time-Of-Flight walls of the ELAN experiment previously carried out at ELSA in Bonn.
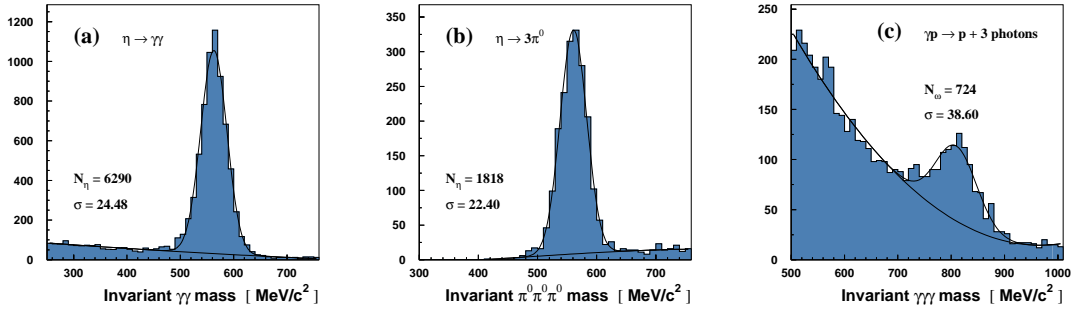
FIGURE 3. **Invariant 2γ mass (a), 6γ mass (b) and 3γ mass (c):** *beam energy: $E_{e^-} = 2.6\ GeV$*

The latter form together with the tagging system and the inner detector the first-level trigger of the experiment. The second level then consists of a fast cluster encoder which is able to determine the number of clusters in the barrel.

FIRST PRELIMINARY RESULTS OF SPECIFIC REACTIONS

Data has been taken since December 2000 with the whole apparatus fully operating. Measurements at three different ELSA energies have been performed: $E_0 =$1400, 2600 and 3200 MeV. In the following, first results on the reactions $\gamma p \rightarrow p\pi^0\pi^0$ and $\gamma p \rightarrow p\pi^0\eta$ are presented. The whole data sample for these reactions comprises about 60 % of the $E_0 = 3200$ MeV data resulting in 150 000 and 20 000 events, respectively. It has to be pointed out that all distributions are neither efficiency corrected nor any flux normalisation has been carried out. However, the reconstruction efficiency is almost flat in cosθ (of the proton in the center-of-mass system) and energy. Furthermore, no final tracking has been performed, therefore, improvements can be expected.
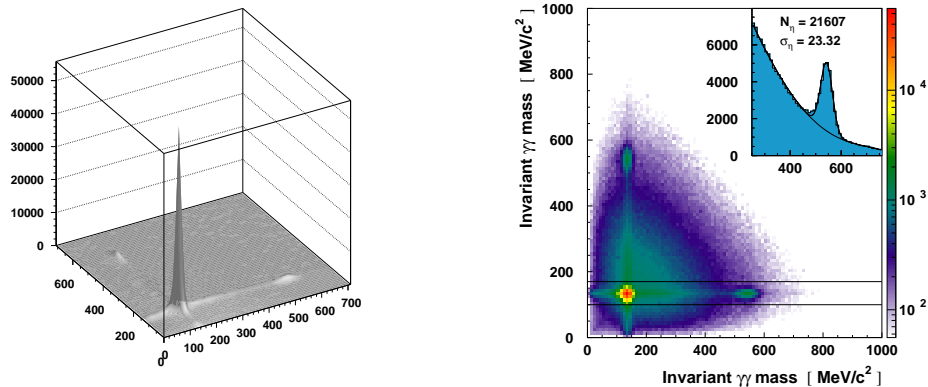
FIGURE 4. **proton + 4γ events: invariant γγ mass versus γγ mass** *(all combinations are plotted)*
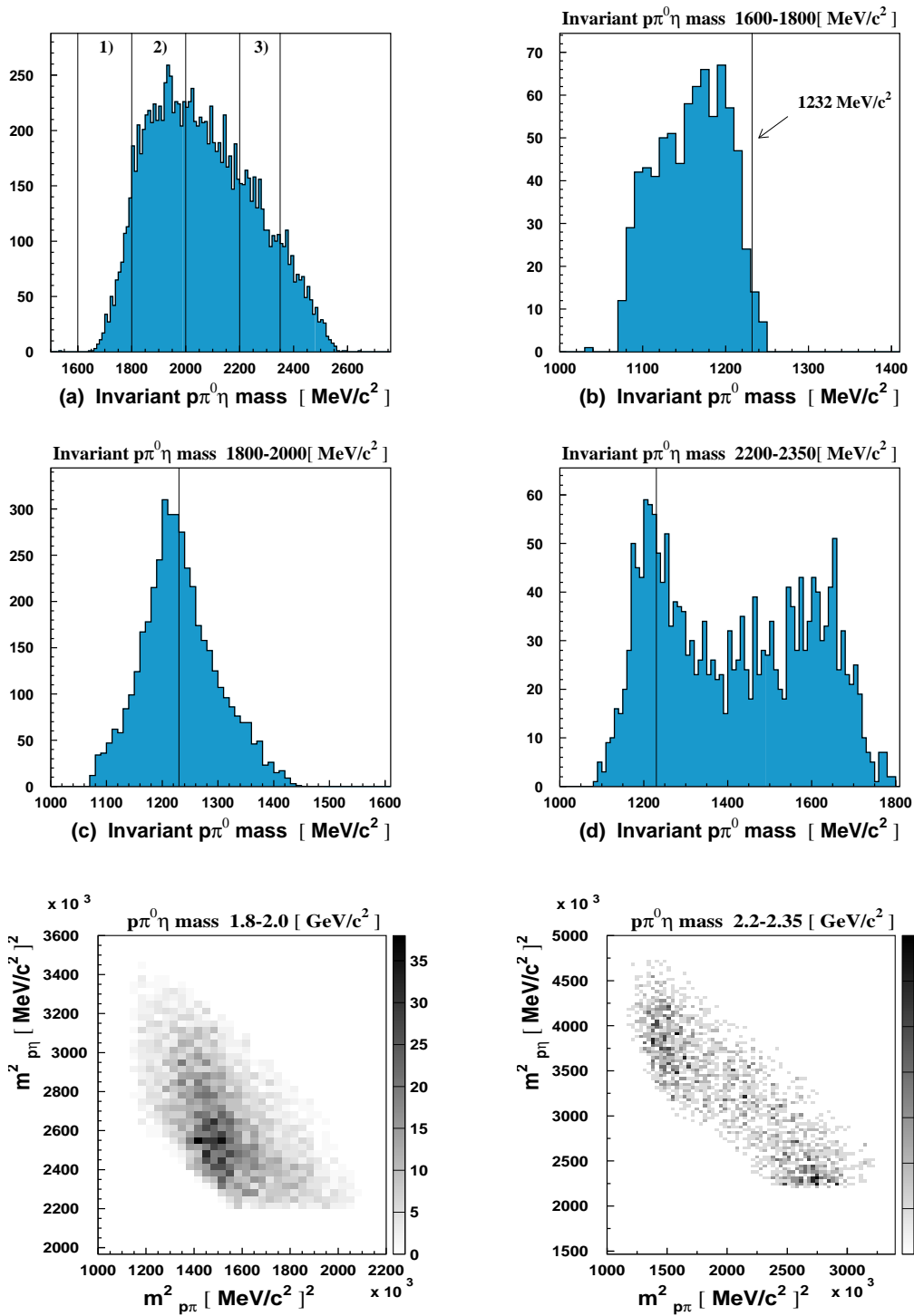
FIGURE 5. **Different plots on the reaction** $\gamma p \rightarrow p\pi^0\eta$**.** *(a) shows the total invariant $p\pi^0\eta$ mass. In (b)-(d), the $p\pi^0$ mass is plotted for the three different $p\pi^0\eta$ mass regions indicated in (a). Clear evidence for the $\Delta(1232)$ can be observed and, thus, hints for resonances decaying via $\Delta\eta$ become obvious. (e) and (f) show Dalitz plots for two different $p\pi^0\eta$ mass regions. Resonance structures become even more transparent.*

The good quality of the data can be seen in Fig. 3 (a) and (b) showing the invariant $\gamma\gamma$ mass as well as the invariant $3\pi^0$ mass, respectively. A clear η signal is visible due to the two neutral decay modes of the reaction $\gamma p \rightarrow p\eta$ above a very small background. No additional constraints have been applied to the events but the request for the right multiplicity identifying the proton with the help of the scintillating fibre detector. Fig. 3 (c) shows the invariant 3γ mass. An ω signal can clearly be seen.

Events with four photons in the final state have to be investigated for the reactions of interest. Fig. 4 shows $\gamma p \rightarrow p\gamma\gamma\gamma\gamma$ events. In the left picture, clear evidence for $\pi^0\pi^0$ events can be observed. However, a small enhancement in the region of $\pi^0\eta$ events is already visible. The latter become more obvious in the right picture using a logarithmic scale in the third direction. In addition, a horizontal cut is applied and the corresponding slice projected onto the x axis (small inset).

$$\gamma p \rightarrow p\pi^0\eta$$
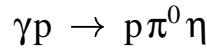
Fig. 5 (a) shows the total invariant mass for the $p\pi^0\eta$ final state. No structures are visible at first sight. However, if one looks at the invariant $p\pi^0$ mass for different total mass regions, hints for baryon resonances decaying into $\Delta\eta$ become visible.
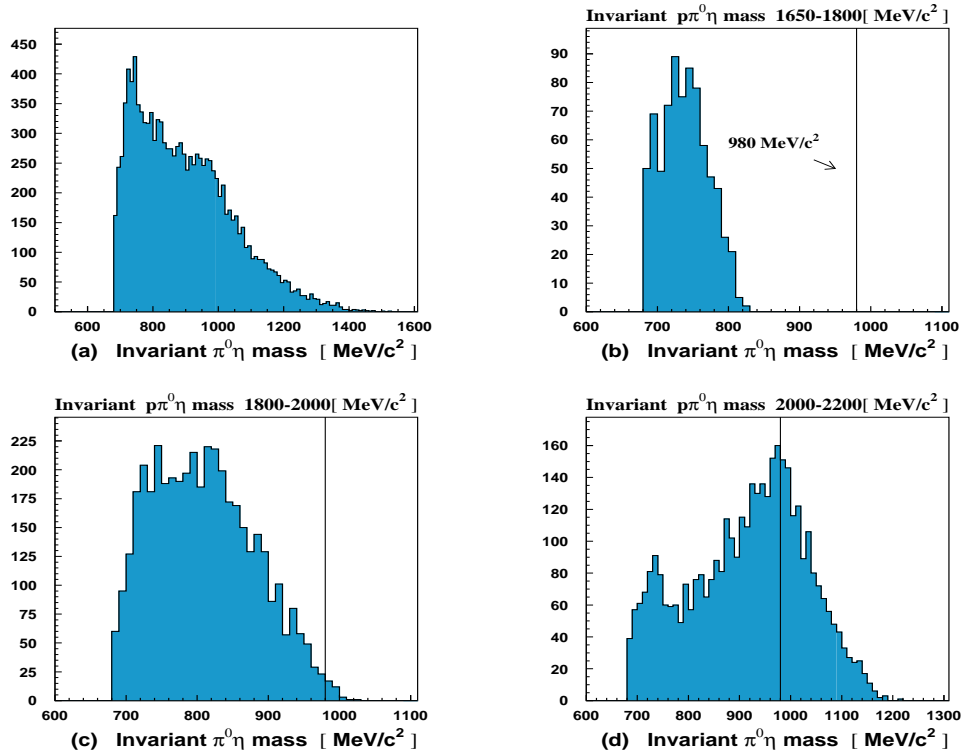
FIGURE 6. **Different plots on $\pi^0\eta$ mass distributions of $\gamma p \rightarrow p\pi^0\eta$.** *(a) shows the $\pi^0\eta$ mass for all events. A bump at 980 MeV can be seen. In (b)-(d), the $\pi^0\eta$ mass is plotted for the same $p\pi^0\eta$ mass regions as indicated in Fig. 5(a). The $a_0(980)$ threshold is at $E_\gamma = 1449$ MeV.*

Fig. 5 (b), (c) and (d) correspond to the three different mass regions which are indicated in (a). In the total mass region around 1700 MeV, no structure can be seen. However, a clear peak at the Δ mass can already be observed in the mass region around 1900 MeV. This might be a first indication for the $\Delta(1940)D_{33}$ decaying into $\Delta\eta$. For higher $p\pi^0$ masses, further resonance intensity may be hidden in a structure around 1600 MeV. In fact, one has to be careful interpreting structures in the mass projections as those are often reflections of the corresponding Dalitz plots (Fig. 5 (e) and (f)).

Fig. 6 (a) shows the invariant $\pi^0\eta$ mass originating from mass projections of the diagonal bands of the Dalitz plot onto the $\pi^0\eta$ axis. The pictures (b), (c) and (d) represent the same three total mass regions as indicated in the $p\pi^0\eta$ mass spectrum. Possibly, a signal for the $a_0(980)$ can be observed above threshold (d). In any case, further investigation may help to shed some light on the structure of this meson which appears in some theoretical scenarios to be a $K\overline{K}$ molecule whereas it is also discussed as a normal quark-antiquark state.
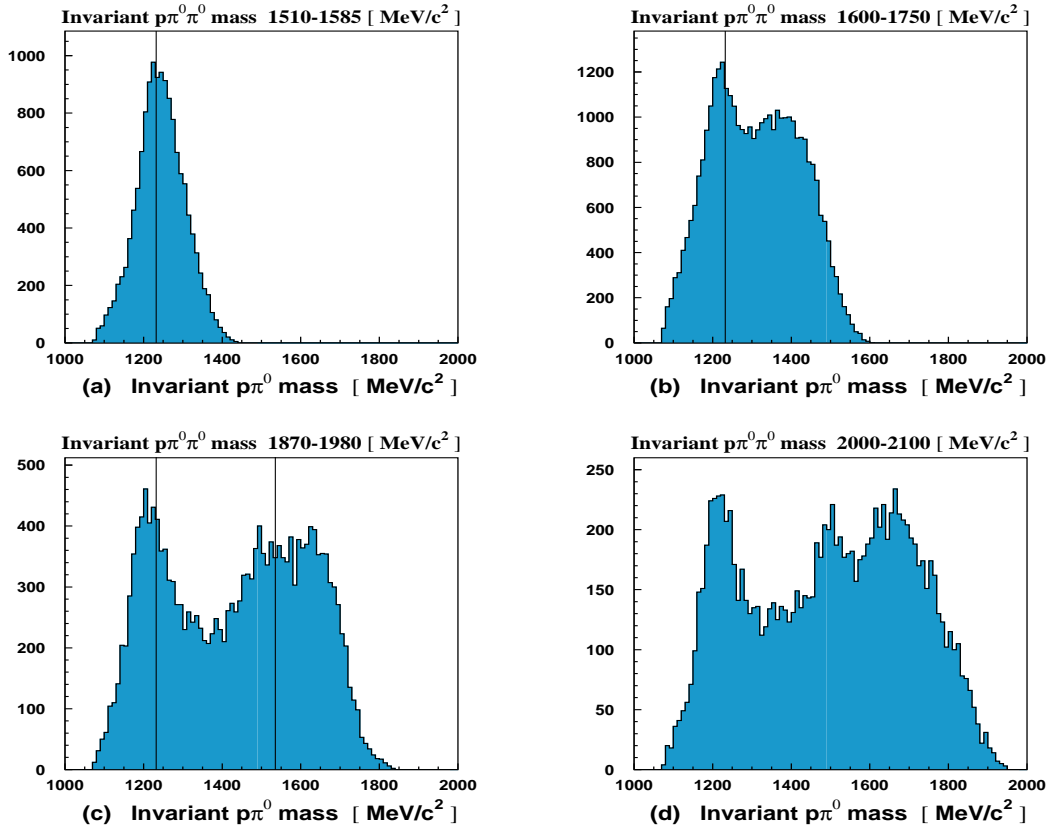
FIGURE 7. **Different plots on the reaction** $\gamma p \rightarrow p\pi^0\pi^0$. *(a)-(d) show the $p\pi^0$ mass for different $p\pi^0\pi^0$ mass regions of the overall distribution (Fig. 8). A clear peak for the $\Delta(1232)$ is observed indicating baryon resonances decaying via $\Delta\pi^0$. However, at higher energies even more structures become visible. These are promising hints for* missing resonances.
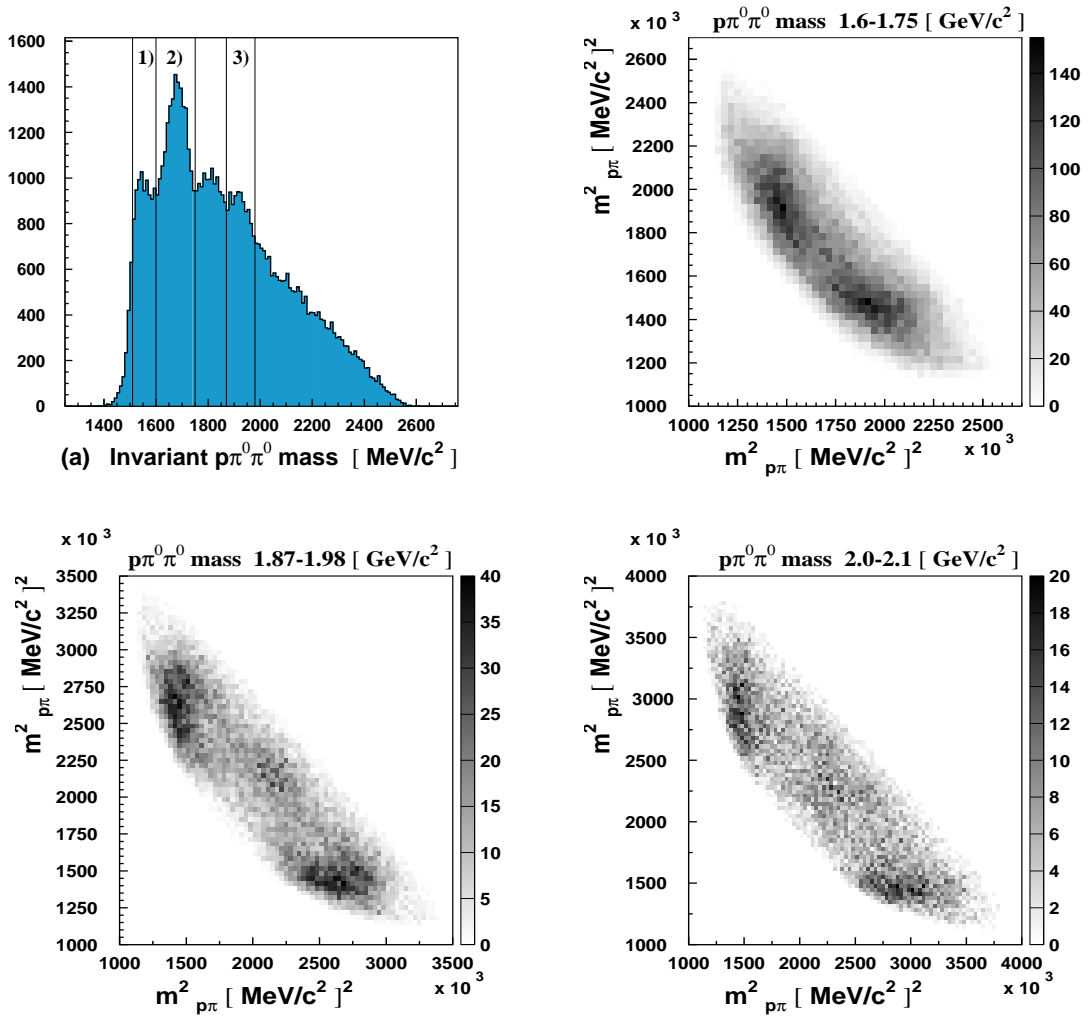
FIGURE 8. Total invariant $p\pi^0\pi^0$ mass (a) and Dalitz plots for the indicated mass regions (b)-(d).

$$\gamma p \rightarrow p\pi^0\pi^0$$

In comparison to the reaction discussed above, structures are already visible in the total invariant $p\pi^0\pi^0$ mass spectrum (Fig. 8). A dominant signal around 1500 MeV is suppressed in the 3.2 GeV data set because it lies below the threshold that can be reached with these data. However, it can clearly be seen in data stemming from incoming electrons with $E_0 = 2.6$ GeV. Following the same idea as before, different mass regions are indicated. The corresponding $p\pi^0$ mass spectra are given in Fig. 7 and 8. In the mass region below 1600 MeV only a single signal for the Δ can be observed. Going higher in mass, an additional signal around 1500 MeV and further structures above 1600 MeV become visible. In fact, the structure around 1500 MeV is very likely to be the $D_{13}(1520)$.

SUMMARY AND CONCLUSION

The preliminary results of the first series of measurements with the Crystal-Barrel experiment at ELSA show promising hints that the data will shed some light on the miracle of the *missing resonances*. The good quality of the data in various channels is convincing and resonance structures even at higher masses are visible.

In the $p\pi^0\pi^0$ channel, clear evidence is given for resonance structures decaying via $\Delta(1232)\pi^0$ at different masses between 1500 MeV and 2100 MeV. In addition, the $p\pi^0$ mass distributions (Dalitz plots) give promising hints that decays via $D_{13}(1520)$ and also via higher-mass baryon states (m > 1600 MeV) are observed.

In the $p\pi^0\eta$ channel, decays of baryon resonances via $\Delta(1232)\eta$ with different masses are obvious. Furthermore, decays via $S_{11}(1535)\pi^0$ are seen and even $a_0(980)$ production may have been observed.

Further effort is necessary in order to obtain final results on baryon resonances and their properties, i.e. to improve the reconstruction of data and to perform partial wave analyses. However, the observed baryonic cascades $B^{**} \to B^*\pi^0 \to p\pi^0\pi^0$ as well as $B^{**} \to B^*\pi^0(\eta) \to p\pi^0\eta$ have never been seen before at this precise level and will reveal a series of new physics results.

REFERENCES

1. L.Y. Gloszman and D.O. Riska: Phys. Rept. **268** (1996) 263
2. S. Capstick and N. Isgur: Phys. Rev. **D34** (1986) 2809
3. U. Löhring, K. Kretzschmar, B.Ch. Metsch and H.R. Petry: EPJ **A10** (2001) 309
4. D.B. Lichtenberg: Phys. Rev. **178** (1969) 2197
5. E.S. Ackleh, T. Barnes and E.S. Swanson: Phys. Rev. **D54** (1996) 6811
6. A.Le Yaouanc, L. Oliver, O. Pene and J.C. Raynal: Phys. Rev. **D18** (1978) 1591
7. S. Capstick and W. Roberts: Phys. Rev. **D49** (1994) 4570; Phys. Rev. **D57** (1998) 4301; Phys. Rev. **D58** (1998) 074011
8. N. Isgur and G. Karl: Phys. Rev. **B72** (1977) 109
9. N. Kaiser, P.B. Siegel and W. Weise: Phys. Lett. **B362** (1995) 23
10. G. Höhler: PiN Newslett. **14** (1998) 168
11. D. Husmann and W.J. Schwille: Phys. Bl. **44** (1988) 40